IEEE Access
Multidisciplinary | Rapid Review | Open Access Journal

Received October 31, 2018, accepted November 13, 2018, date of publication November 26, 2018,
date of current version December 31, 2018.

Digital Object Identifier 10.1109/ACCESS.2018.2883379

Highly Efficient Wearable CPW Antenna Enabled by EBG-FSS Structure for Medical Body Area Network Applications

ADEL Y. I. ASHYAP[1], ZUHAIRIAH ZAINAL ABIDIN[1], (Member, IEEE), SAMSUL HAIMI DAHLAN[1], (Member, IEEE), HUDA A. MAJID[1], (Member, IEEE), MUHAMMAD RAMLEE KAMARUDIN[2], (Senior Member, IEEE), AKRAM ALOMAINY[3], (Senior Member, IEEE), RAED A. ABD-ALHAMEED[4], (Senior Member, IEEE), JAMAL SULIEMAN KOSHA[4], (Senior Member, IEEE), AND JAMES M. NORAS[4]

[1]Center for Applied Electromagnetic, Faculty of Electrical and Electronic Engineering, Universiti Tun Hussein Onn Malaysia, Batu Pahat 86400, Malaysia
[2]Centre for Electronic Warfare, Information and Cyber, Cranfield Defence and Security, Cranfield University, Defence Academy of the United Kingdom, Shrivenham SN6 8LA, U.K.
[3]Antennas and Electromagnetics Research Group, School of Electronic Engineering and Computer Science, Queen Mary University of London, London E14NS, U.K.
[4]Faculty of Engineering and Informatics, University of Bradford, Bradford BD7 1DP, U.K.

Corresponding authors: Zuhairiah Zainal Abidin (zuhairia@uthm.edu.my) and Muhammad Ramlee Kamarudin (ramlee.kamarudin@cranfield.ac.uk)

This work was supported in part by the Ministry of Education Malaysia (MOE) under Research Accularation Collaborative Effort (RACE) Vot No. 1510 and GPPS Vot. No. U739.

ABSTRACT A wearable fabric CPW antenna is presented for medical body area network (MBAN) applications at 2.4 GHz based on an electromagnetic bandgap design and frequency selective surface (EBG-FSS). Without EBG-FSS, the basic antenna has an omnidirectional radiation pattern, and when operated close to human tissue, the performance and efficiency degrade, and there is a high specific absorption rate. To overcome this problem, the antenna incorporates EBG-FSS, which reduces the backward radiation, with SAR reduced by 95%. The gain is improved to 6.55 dBi and the front-to-back ratio is enhanced by 13 dB compared to the basic antenna. The overall dimensions of the integrated design are $60 \times 60 \times 2.4$ mm^3. Simulation and experimental studies reveal that the antenna integrated with EBG-FSS can tolerate loading by human tissue as well as bending. Thus, the design is a good candidate for MBAN applications.

INDEX TERMS AMC, EBG, SAR, wearable fabric antennas.

I. INTRODUCTION

Medical Body Area Networks (MBAN) are becoming a vital technology in wearable systems, with applications in telemetry and medicinal services. MBAN is utilized to observe the health of patients at home, in hospital or even at outpatient surgeries. The important parameters of health are measured using implanted and wearable systems, which permit a continuous and unobtrusive examination of patients' state of health, for example monitoring blood pressure, ECG, EEG, or heart rate. The performance of the MBAN relies on the efficiency of the wireless communication devices, which need to be light-weight, low-profile, miniaturized, efficient, flexibly conforming to the shape of the human body, and capable of giving continuous monitoring. They must also ensure dependable communication within their networks.

The antenna is key to the wireless communication system and dictates its operation. Designing narrowband and robust wearable antennas, with acceptable efficiency and performance is a challenging task, particularly when the antennas are expected to possess lightweight, low-profile and conformal characteristics [1]–[11].

Positioning the antenna near a lossy medium such as the human body causes performance reduction, since capacitive coupling between the human body and the antenna alters the operating frequencies and the input impedance of the antenna. Also, the radiation efficiency of the antenna is expected to diminish due to the absorption of some power by the body tissue, and changes in the radiation pattern can result in transmission errors [8]–[10]. In order to be useful in MBAN, antennas must be able to function well close to human tissue,

with very low radiation toward the body to meet the specific absorption rate (SAR) limit.

To date, quite a few wearable antennas have been introduced operating at the demand frequency of 2.4 GHz, with and without the integration of flexible materials. Aside from coplanar waveguide (CPW) antennas [12]–[14], traditional patches, slot patches and monopole antennas [15]–[18], subsequent versatile antenna designs with improved efficiency and performance have appeared. Magneto-electric dipole antennas [19] and substrate-integrated waveguide antennas [20]–[23] have been designed based on fabric materials, showing either dual-band or single-band operation. At the same time, monopoles [24] and inverted-F fabric antennas [25], [26] have been well documented. They are small in area, yet may increase SAR levels when working near to body tissue, because of their nearly bi-directional radiation patterns. In an endeavor to diminish the effect of human tissue loads and enhance the isolation, High Impedance Surface (HIS) designs have been presented and implemented using either semi-flexible or flexible materials [27]–[36]. The HIS designs attain high degrees of isolation between the antennas and the body tissues. However, these proposed designs have the drawbacks of large footprints and may be too thick and big for MBAN applications [27]–[33], use semi-flexible material that is not adequately bendable and may not be comfortable for users [34], [35]. They may also show a frequency shift due to bending or poor front to back ratio (FBR) [29], [32], [36].

Generally, electromagnetic wave radiation is deemed unsafe for human tissue health. Furthermore, when an antenna is near to the body, it is influenced by the human body's biological organization. Therefore, there are strict standards for SAR defined for Europe or the US to follow.

Accordingly, to reduce SAR below the safety limits, an electromagnetic band-gap (EBG) has been used [27]–[36], since EBG could eliminate most of the electromagnetic energy in the desired frequency bands. In this study, a fabric CPW antenna integrated with EBG-FSS structures is designed and studied to determine its benefits and safety. The antenna incorporating EBG-FSS is thinner than those in previous work as compared in Table 1 [27]–[36]; in addition, its SAR values are reduced significantly and the antenna gain enhanced.

This paper is arranged as follow: Section II discusses the CPW antenna and EBG designs, with CST software [37] employed in examining the antenna's size and electric properties; Section III covers the integration of the CPW antenna with EBG and investigates performance in free space as well as the impacts of placing EBG and PEC over the antenna; Section IV considers the behavior of the design when it is bent and loaded on the human body, with distances between the design and tissues varied to study the impacts on performance and SAR; finally Section V concludes with the achievements of the design.

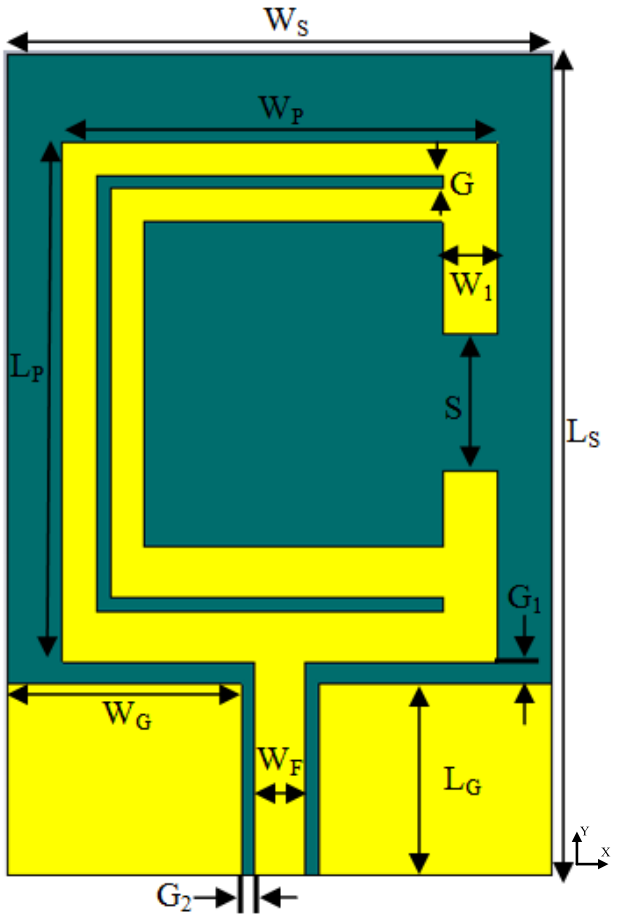

FIGURE 1. Front view of the fabric CPW antenna. The optimized dimensions are $L_S = 30$ mm, $Ws = 20$ mm, $Wp = 16$ mm, $Lp = 19$ mm, $W_1 = 2$ mm, $G = 0.5$ mm, $G_1 = 0.8$ mm, $G_2 = 0.5$ mm, $S = 5$ mm, $LG = 7$ mm, $W_G = 8.57$ mm, and $W_F = 1.86$ mm.

II. DESIGNS OF ANTENNA AND EBG STRUCTURES

A. DIMENSION AND SIZE DESIGN

A wearable textile antenna is designed as shown in Fig. 1. It is C-shaped, additionally etched with a C-slot. This slot on the radiator element is to obtain compactness in size. A coplanar waveguide is fed at the bottom of the substrate, with a signal strip of width W_F and two gaps of G_2. Two rectangular patches beneath the radiating elements support the antenna as ground planes. The CPW feeding method reduces the fabrication complexity of the antenna, because both the ground planes and the radiator are positioned on the top of the dielectric.

Jeans material (denim) with a thickness of 0.7 mm, a loss tangent of 0.07 and a relative permittivity of 1.7 provided the supporting dielectric substrate. To achieve 50 Ω characteristic impedance, the size of the width W_F, the gap G_2, and other dimensions are critical. The overall size of the antenna is $30\times20\times0.7$ mm^3. The working frequency band was selected as 2.4 GHz for MBAN applications.

TABLE 1. Comparison of previous wearable antenna with presented design.

Ref	Number of unit cell	Gain (dBi)	Dimensions (mm3)	Bandwidth (%)	SAR(w/kg) 1 g	10 g	Distance from the body	Reflected plane	Substrate type
[27]	6× 4	7	318×212×7	9.52	N/A	N/A	N/A	AMC	Felt/flexible
[28]	3×3	6.4	120 ×120 ×4.3	4	0.079	0.043	5.3	EBG	Felt/flexible
[29]	3×3	7.3	81×81×4	14.7	0.554	0.2	6	EBG	Felt /Flexible
[30]	3×3	N/A	150 ×150×4	5.08	N/A	0.016	1	EBG	Jeans / Flexible
[31]	2×2	5.2	50×50×5	11.3	0.13-0.18	N/A	4	HIS	PDMS/ Flexible
[32]	3 × 3	4.8	65.7×65.7× 3.3	18	0.683	N/A	N/A	AMC	Kapton polyimide for antenna and viny for AMC/ Flexible
[33]	3 × 3	N/A	72×72×5	9.2	1.57	0.37	N/A	Metamaterial	Polyimide/ Flexible
[34]	1×2	6.88	68×38× 6.57	5	0.244	N/A	2	EBG	RT/duroid 5880 /Semi-flexible
[35]	2×2	6.2	62 × 42 × 4	5.5	0.79	N/A	1	Metsurface	Rogers RO3003 /Semi-flexible
[36]	4 × 4	2.5	100×100×4.5	N/A	N/A	0.0464	10	AMC	Felt/Flexible
This paper	2×2	6.55	60×60×2.4	8.3	0.055	N/A	1	EBG-FSS	jeans/flexible

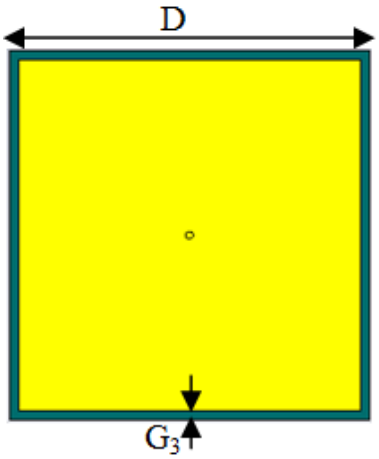

FIGURE 2. Conventional Sievenpiper EBG. The optimized dimension is D = 48 mm, G_3 = 1.2 mm and via = 0.5 mm.

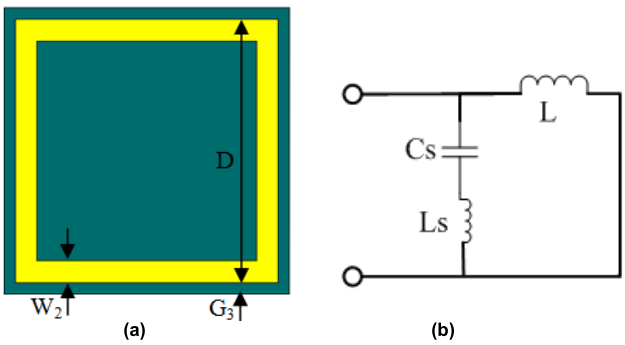

FIGURE 3. (a) Square loop based on EBG-FSS and (b) equivalent circuit of (a). The optimized dimensions are D = 27.6 mm, G_3 = 1.2 mm, and W_2 = 2.25 mm.

B. SQUARE LOOP EBG STRUCTURE

The traditional Sievenpiper EBG is illustrated in Fig. 2. The desired frequency is calculated based on equation (1) [38]. It is realized that the unit cell has an overall dimensions of 48×48×0.7 mm^3. In order to form an array of 2×2, the overall dimension will increase to 96 ×96×0.7 mm^3. This dimension is considered electrically large; therefore, it is desired to reduce the conventional dimensions.

$$f = \frac{1}{2\pi\sqrt{LC}} \tag{1}$$

An increment in the capacitance or the inductance of the structures lowers the frequency. However, increasing the capacitance diminishes the bandwidth. Hence, it is better to increase the inductance instead of the capacitance of the structure. The inductance can be increased without increasing the capacitance by using a thick substrate, but a thicker substrate takes more space and enlarges the systems. A different approach is to employ a frequency selective surface (FSS) through a series LC equivalent circuit model rather than a traditional patch. In this case, the desired frequency is given by equation (2) [32], [39], which shows that the total structural inductance increases due to the additional surface inductance. Hence, it is necessary to use the high-inductance FSS as a top layer rather than a traditional patch that behaves as a capacitive surface. A design that has this type of model with significant inductance is called a square loop, and is shown in Fig. 3(a) [39]. Note that there are several FSS structures with series LC models that have a significant inductance. However, the majority of structures are complex or have vias, and vias and complexity are not preferable in designing for fabric materials and might lead to inaccuracy.

$$f = \frac{1}{2\pi\sqrt{(L + L_s)\,C_s}} \tag{2}$$

A demonstration of 2×2 array square loop FSS-EBG has been studied and verified through simulation and measurement of an equivalent circuit. The finite integrated method is used to design this EBG-FSS structure in CST. In order

to have a low-profile design, the EBG-FSS is constructed on 0.7 mm thickness of denim, the same as the CPW antenna substrate. The equivalent circuit model of the designed textile square-loop is inspired from [32], [35], and [39]–[41] as illustrated in Fig. 3(b). It is an LC series circuit where the capacitance (Cs) is due to the gap size between horizontal conductor and calculated by the following equation (3) [3], [42].

$$C_S = \frac{W\varepsilon_0\,(1+\varepsilon_r)}{\pi}\cosh^{-1}\left(\frac{W+g}{g}\right) \tag{3}$$

where W is the perimeter dimensions of the unit-cell conductive material, and g is the gap size between the two adjacent unit-cells.

The inductance (Ls) comes from the loop metal conductors and calculated by the following equation (4) [43].

$$L_S = \ell_n \frac{\mu_0}{4\pi}\ln\left\{1+\frac{32h^2}{w_n^2}\left[1+\sqrt{1+\left(\frac{\pi w_n^2}{8h^2}\right)^2}\right]\right\} \tag{4}$$

where ℓ is the length of the strip, h is the substrate thickness and w is the width of the strip.

The inductance L is the load and given by the following equation [42].

$$L = \mu_0 h \tag{5}$$

where μ is permeability, h is the substrate.

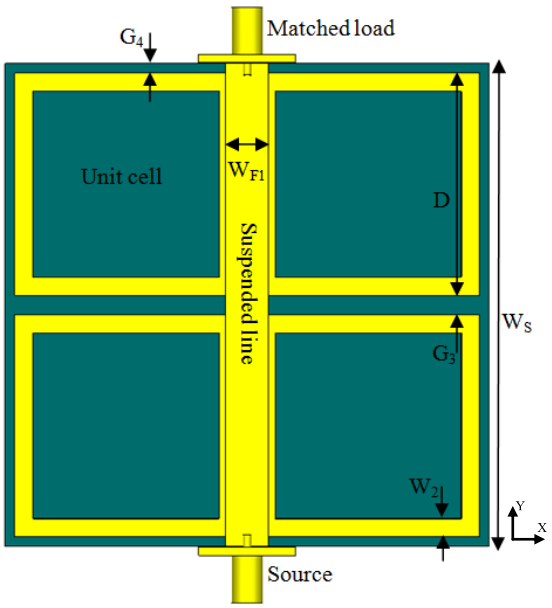

FIGURE 4. Technique of suspended microstrip line to evaluate band-gap. The optimized dimensions are Ws =60 mm, D = 27.6 mm, G_3 = 2.4 mm, G_4 = 1.2 mm, W_2 = 2.25 mm, and W_{F1} = 5.32 mm.

The technique of a suspended microstrip line [44] is utilized to study the band-gap features of the square loop EBG-FSS structures, as depicted in Fig. 4. The EBG-FSS array is placed between the suspended line and ground, forming a sandwich-like structure. The suspended line is placed between two waveguides during simulation and soldered with two SMA connectors during measurements to evaluate the S_{21} parameters. Compared with traditional monopoles and coplanar microstrip techniques, the suspended line is a robust coupling structure, lessening the impact of other parasitic propagation modes. The band-gap features of the EBG-FSS are revealed more clearly.

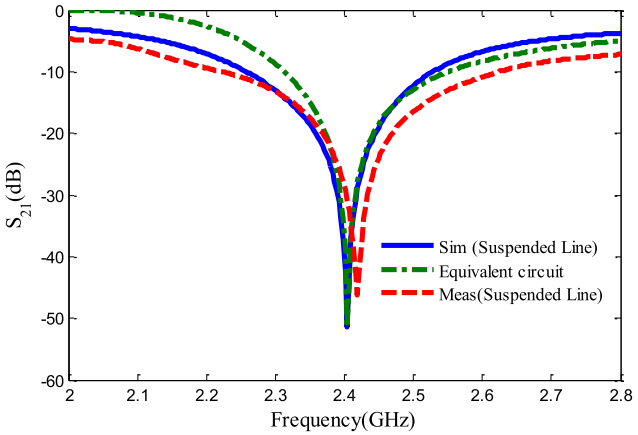

FIGURE 5. S_{21} band-gap characteristics based on suspended line technique and equivalent circuit.

Fig. 5 depicts the comparative results of the EBG-FSS unit cell based on the suspended line technique with the equivalent circuit, which is the result of the equivalent circuit is obtained from the ADS software. Only S_{21} is shown for clarity. A particular stop-band is seen with resonant frequency of 2.4 GHz. The range of frequency with S_{21} less than -10 dB [45] extends for the three cases from 2.25 GHz to 2.53 GHz.

III. INTEGRATION OF ANTENNA WITH EBG-FSS

A. ANTENNA PERFORMANCE WITH EBG-FSS

Once the textile CPW antenna and EBG-FSS have been designed separately, the textile CPW antenna is combined with EBG-FSS, using as a separation between them 1 mm thick foam, with permittivity of 1.05 and loss tangent of 0.0003. This separation is optimum, giving the antenna integrated with EBG-FSS the best S_{11}. Fig. 6(a) illustrates the configuration of the integrated design.

Note that with the antenna placed over the EBG-FSS, a mutual impedance coupling arises between them [46]. This could cause detuning of the resonant frequency. Therefore, to obtain the desired resonant frequency as well as a better reflection coefficient, the dimension of the radiation patch is modified as seen in Fig. 6(b). Here the length of the patch Lp is reduced by 3 mm, W_1 by 1 mm and S is increased by 1.5 mm. Fig. 7 illustrates the simulation and measurement results of S_{11} of the antenna alone and when placed on EBG-FSS. The figure shows sensible agreement between simulated and measured results below -10 dB. There is a slight shift in the measured S_{11} to higher frequency in the case of antenna with EBG-FSS and a slight shift to lower frequency with the antenna alone. This difference could be attributable to the

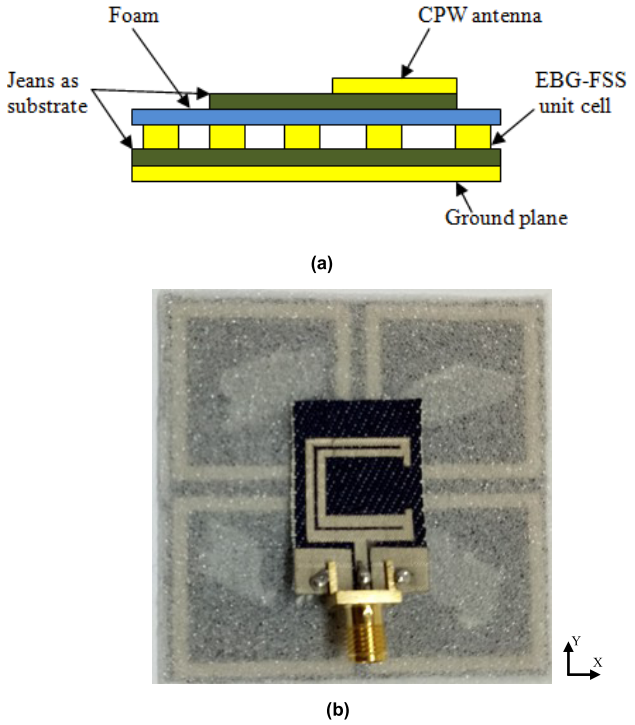

FIGURE 6. Antenna over EBG-FSS: (a) side view of the integrated design and (b) fabricated design.

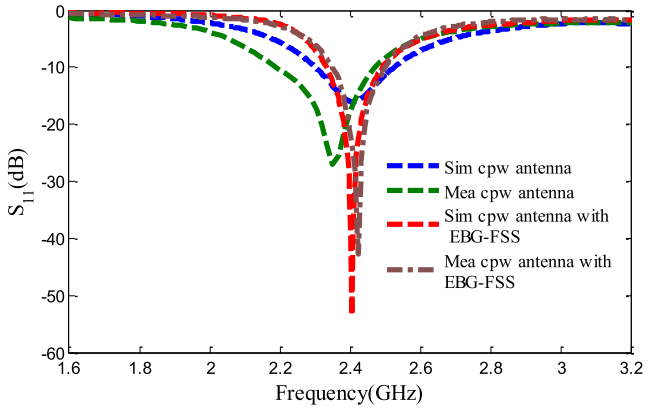

FIGURE 7. CPW antenna with and without EBG-FSS.

accuracy of the fabrication process. Furthermore, integrating antenna with EBG shows better reflection coefficient compared to antenna alone. The result agrees with [29].

The simulation and measurement of the radiation pattern of the antenna with and without the EBG-FSS backing in the H-plane and the E-plane are illustrated in Fig. 8. The experiment was conducted in an anechoic chamber. It is seen that the antenna without EBG-FSS has an omnidirectional pattern in its H-plane and a dipole-like pattern in its E-plane. In other words, the antenna gives maxima along the negative and positive z-axis indicating significant backward radiation. However, integrating the EBG-FSS with the basic antenna leads to a good FBR increase and a higher maximum gain compared with the antenna alone, and decreases the back radiation toward the body by around 13 dB whereas the antenna gain increases from 1.74 dBi to 6.55 dBi, all at 2.4 GHz. Most importantly, the usefulness of the EBG-FSS is achieved without vias and for a small size of 2×2 elements.

B. ANTENNA PERFORMANCE OVER EBG-FSS AND PEC

Experimental studies between the ordinary metal (PEC) and periodic EBG-FSS structure are carried out to show the usefulness of EBG-FSS. Fig. 6(b) and Fig. 9 illustrates the placement of the antenna over EBG-FSS and PEC respectively. To compare fairly, the textile antenna is placed over EBG-FSS and PEC with the same height and dimensions, and in the case of PEC, the experimental studies use the same substrate as EBG-FSS. Fig. 10 displays the experimental results: when the antenna is above PEC as ground plane the reflection coefficient of the antenna has a value greater than -10 dB which almost linear. This is because the ordinary metal surface has 180^0 phase with a $\lambda/4$ spacing between the metal and the antenna, which $\ll \frac{\lambda}{4}$ results in opposing directions of the current of the antenna and the image current of the PEC, causing in a very poor return loss. Furthermore, adding EBG-FSS to the antenna shows a good reflection coefficient at 2.4 GHz. This is due to the phase behavior of the EBG-FSS ensuring that the image current and the original current flow in the same direction giving a constructive result. Overall, the antenna with PEC demonstrates a poorer impedance matching, as indicated by S_{11} greater than -10 while the antenna integrated with EBG-FSS shows much better impedance matching with S_{11} less than -10 dB at 2.4 GHz. Therefore, EBG appears a good choice for a wearable low-profile antenna.

IV. BEHAVIOR OF THE DESIGN ON BODY

A. BENDING EVALUATION

In several applications, the wearable antenna is anticipated to be deformed or conformed to human body surfaces during operation, to make sure that the operating frequency and general characteristics are maintained under bending, as when being worn. Therefore, before examining the human body loading impact, firstly an investigation on the integrated antenna with EBG-FSS under different degrees of structural deformations in free space is desired to ensure its consistency, with curvatures induced using polystyrene cylinders (ε_r) with three different diameters of curvature values, namely 70 80 and 100 mm, as illustrated in Fig. 11. They are chosen based on typical human leg, arm and chest sizes. Adhesive tape is used to fix the antenna on the polystyrene cylinder.

The experimental results of bending along the y-axis (as shown in Fig. 11(a)) with three diameter values are described in Fig. 12(a). It is clear that the desired frequency band and bandwidth are maintained < -10 dB. There is a slight shift to higher frequency operation as the diameter is decreased. With increasing diameter, S_{11} appears more stable as seen in the case of $d = 100$ mm, but overall the

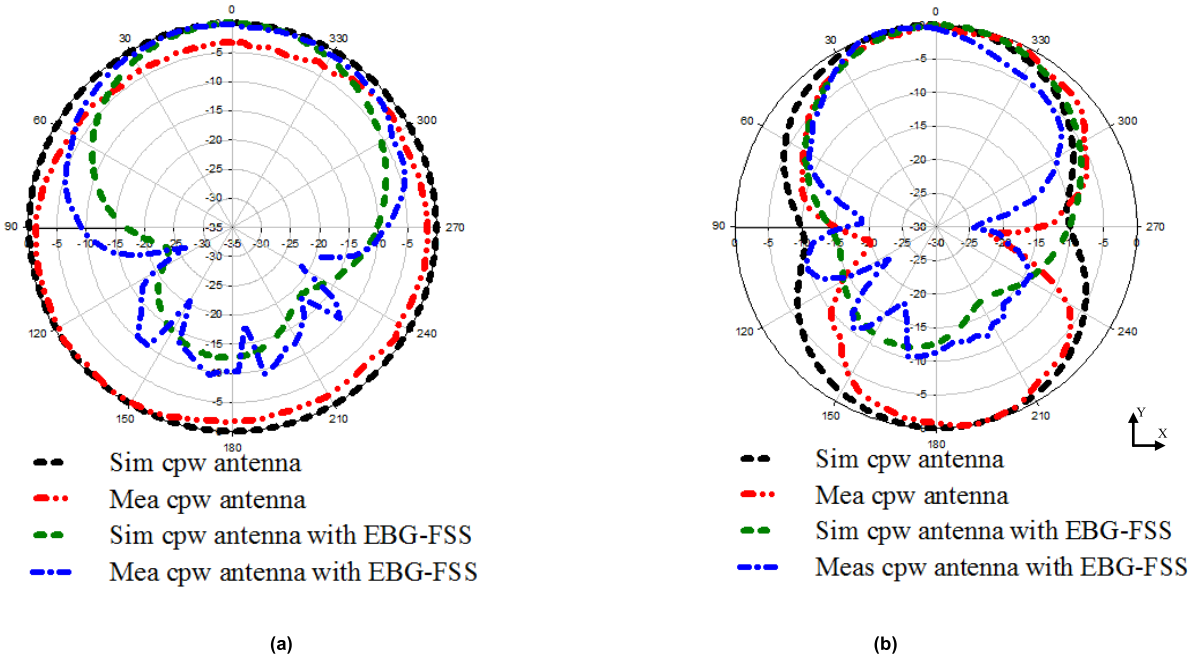

FIGURE 8. The radiation pattern of CPW antenna alone and integrated with EBG-FSS in (a) the H-plane (b) the E-plane.

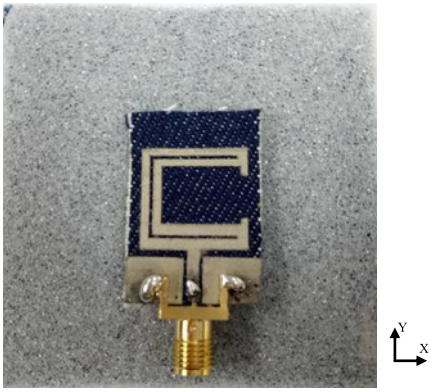

FIGURE 9. Antenna over PEC.

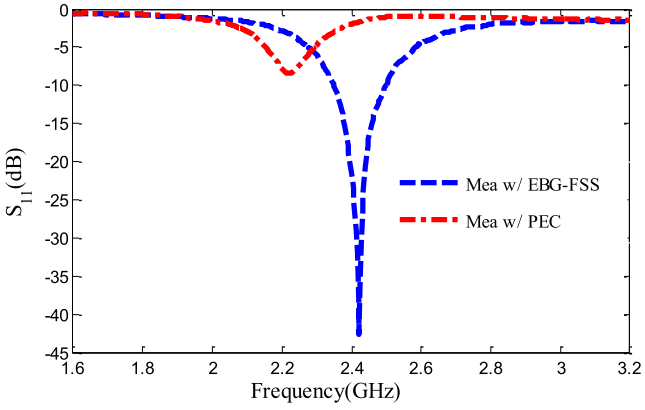

FIGURE 10. Experimental S_{11} of the CPW antenna on EBG-FSS and PEC as ground planes, respectively.

frequency shifts are negligible as the desired frequency band is maintained < -10 dB.

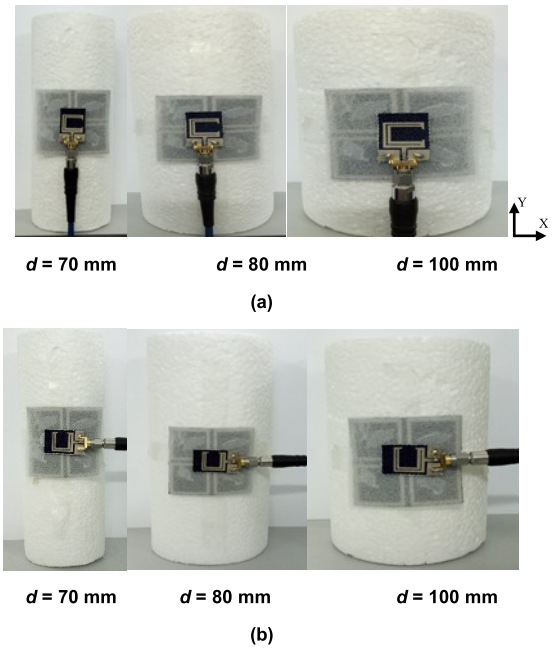

FIGURE 11. Bending process along (a) y-axis and (b) x-axis. (a) $d = 70$ mm $d = 80$ mm $d = 100$ mm. (b) $d = 70$ mm $d = 80$ mm $d = 100$ mm.

Bending along the x-axis is carried out similarly as illustrated in Fig. 11(b). The experimental result is illustrated in Fig. 12(b), and here the effects are greater compared to the case of the y-axis. In case of $d = 70$ mm, the shift is about 30 MHz upwards while with $d = 80$ mm, the shift is about 25 MHz downwards. With $d = 100$ mm the resonant frequency is almost unaffected. Overall, the shifts in frequency

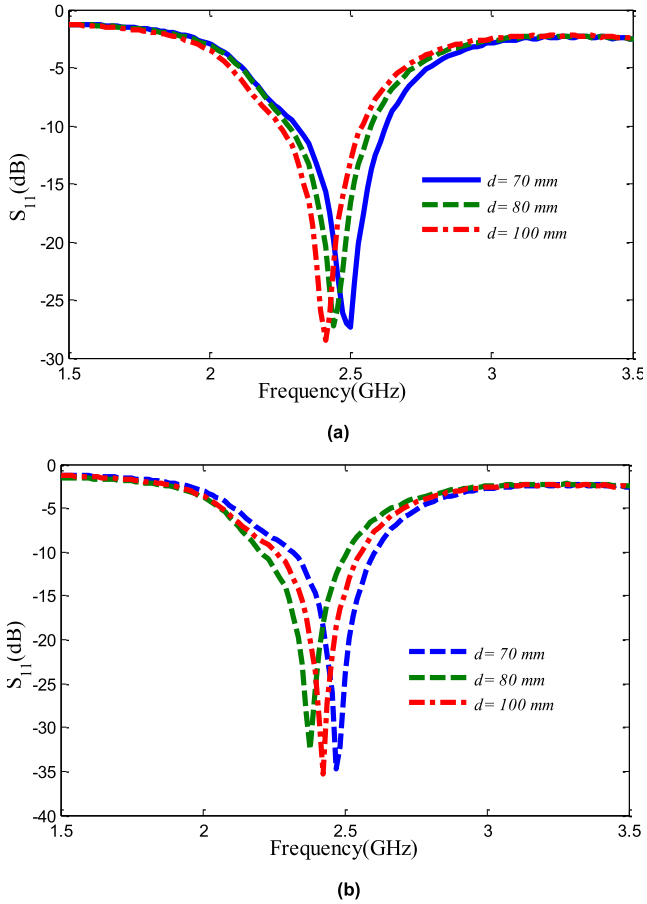

FIGURE 12. Measured S_{11} under bending along (a) y-axis and (b) x-axis.

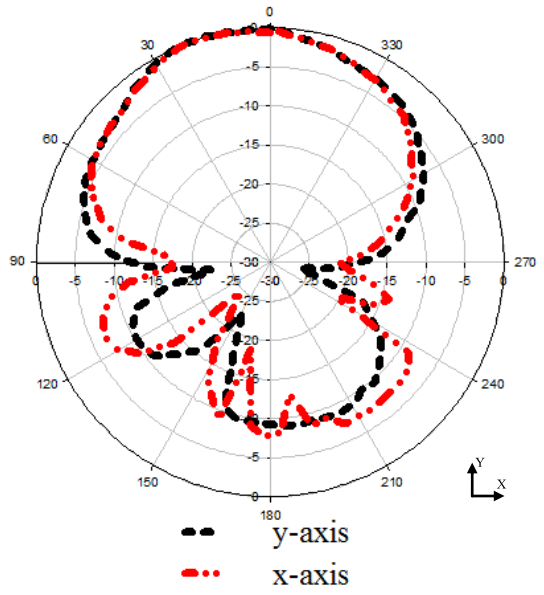

FIGURE 13. Measured radiation patterns under bending with d = 100 mm.

TABLE 2. Properties of the model tissue [35].

	Bone	Muscle	Fat	Skin
Thickness (mm)	13	20	5	2
Density (kg/m^3)	1008	1006	900	1001
σ (S/m)	0.82	1.77	0.11	1.49
ε_r	18.49	52.67	5.27	37.95

still may be considered negligible since the desired frequency still is < -10 dB. The greater effect with the x-axis bending may be due to the current distributions changing along the strip line, affecting the resonant length.

Next, the radiating performance of the antenna integrated with EBG-FSS under bending conditions is investigated. The experimental studies are carried out for one bending direction for each radiating plane. The bending is along the y-axis for the y-plane pattern and along the x-axis for the x-plane pattern with $d = 100$ mm. The integrated antenna was conformably positioned on the cylinder using tape. The experimental results, see Fig. 13, show that the antenna retains good radiating performance, and that the radiating characteristics are insensitive to bending. The bending has a slight effect, namely in increasing the back radiation. The slight asymmetry could be due to the position of the foam separator that may affect the cable movement during the measurement, because of a non-uniformity across the integrated structure during bending.

B. HUMAN TISSUES LOADING EVALUATION

After investigating the integrated antenna in free space, this section studies the impact on performance of human multilayer tissue. The numerical simulation was conducted using CST. A cuboid of $150 \times 150 \times 40$ mm^3 [47] is utilized to emulate the human chest. The model consists of four layers: bone, muscle, fat and skin. Typical mass density, thickness, conductivity, and permittivity values for each layer are tabulated in Table 2 [35]. In our full-wave numerical experiment, the space between the integrated antenna and the tissue models is varied, to understand how the EBG-FSS mitigates the human body's loading effect.

Based on Fig. 14(a), the antenna integrated with EBG-FSS possesses a robust input impedance characteristic with $S_{11} < -10$ dB at the desired frequency, even when it is positioned directly on the multilayer tissue model. S_{11} is very stable with acceptable bandwidth compared to simulation in free space. Conversely, when the antenna is on its own, the impedance performance is sensitive to the separation between the antenna and the tissue. It can be observed that, once the antenna closed to the tissue, S_{11} is most affected, due to the tissue's high dielectric constant of the body. In other words, due to the partial ground of the antenna, the human body is acting as a new complex layer of substrate, therefore mounting the antenna directly on the body causes a dramatic mismatch in the antenna's performance [36].

To validate this, a series of experiments were performed with the antenna with EBG-FSS was directly located on

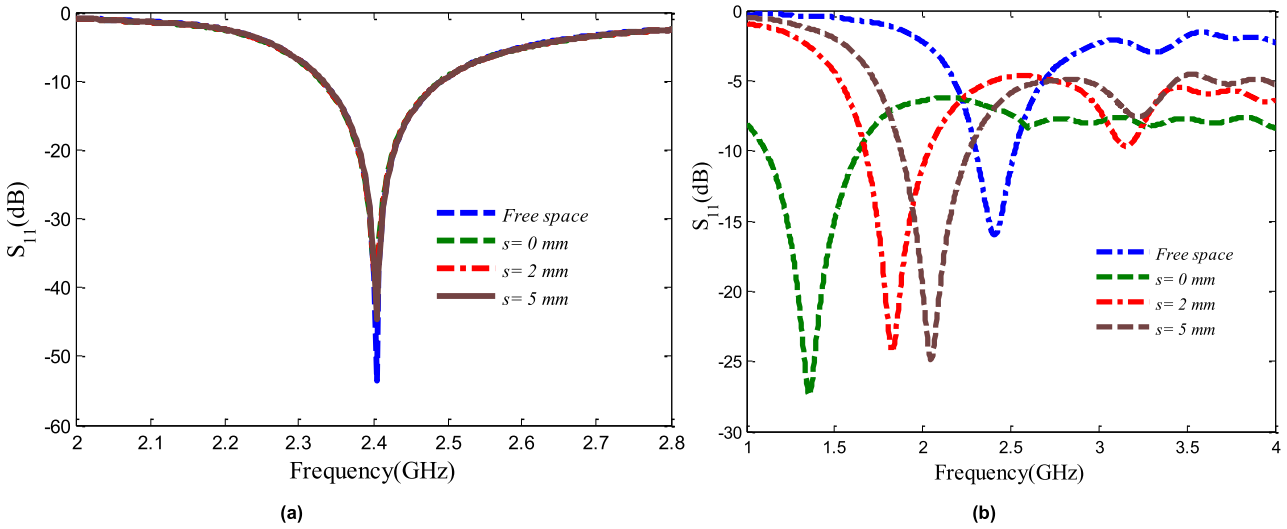

FIGURE 14. Simulated S_{11} behavior for (a) antenna integrated with EBG-FSS and (b) antenna alone on multilayer tissue model representing human chest.

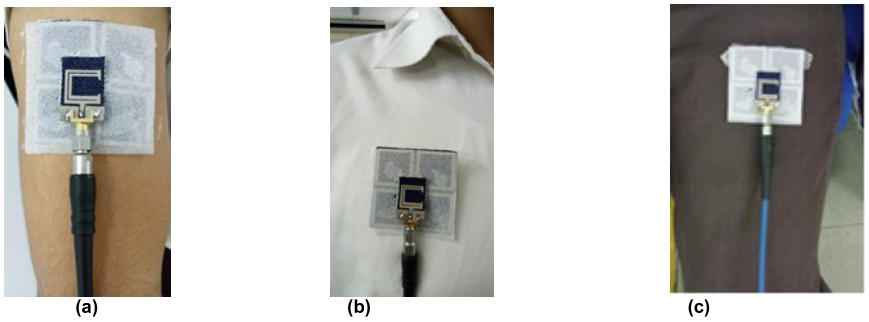

FIGURE 15. Antenna placement on different parts of human body: (a) arm, (b) chest and (c) leg.

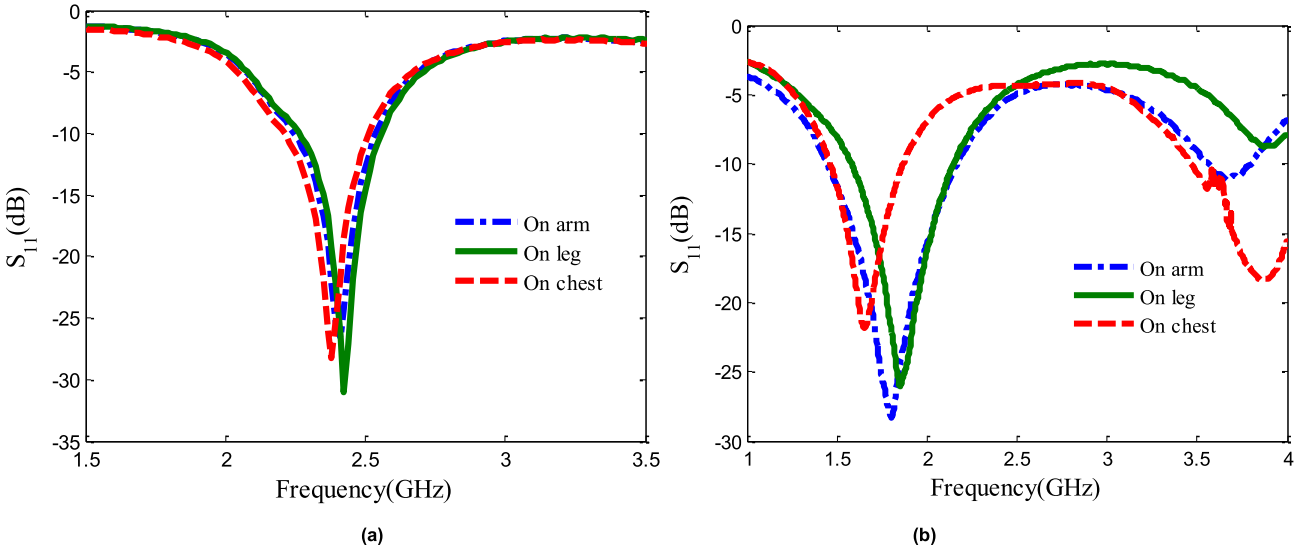

FIGURE 16. Measured S_{11} behavior on human body for (a) antenna integrated with EBG-FSS and (b) antenna alone.

diferent parts of human body such as chest, thigh, and arm as seen in Fig. 15. A male volunteer, weighing 81 kg and height 160 cm, is employed to examine the performance of the prototype design.

In Fig. 16(a), S_{11} is shown for the case of the integrated antenna when located on different parts of the human body. Similar to what we observed in numerical simulation, for the antenna on human chest, the results showed good agreement

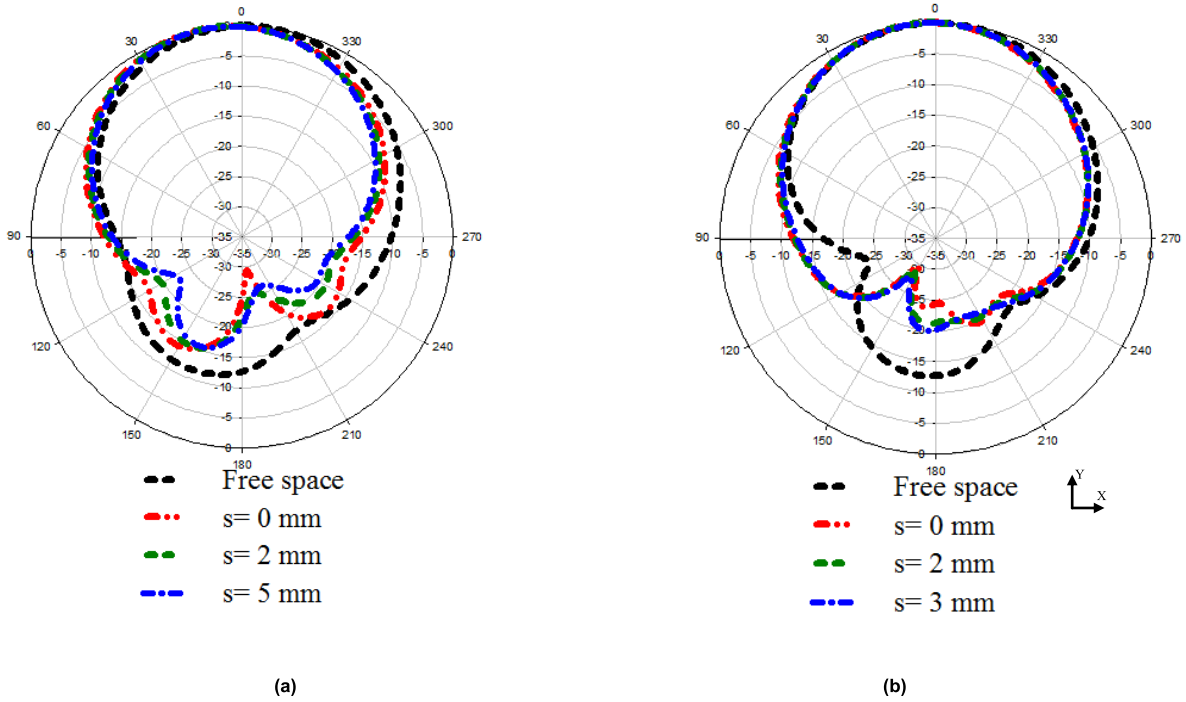

FIGURE 17. Radiation patterns of the integrated antenna with varying distance from the multilayer tissue model in the (a) E-plane and (b) H-plane.

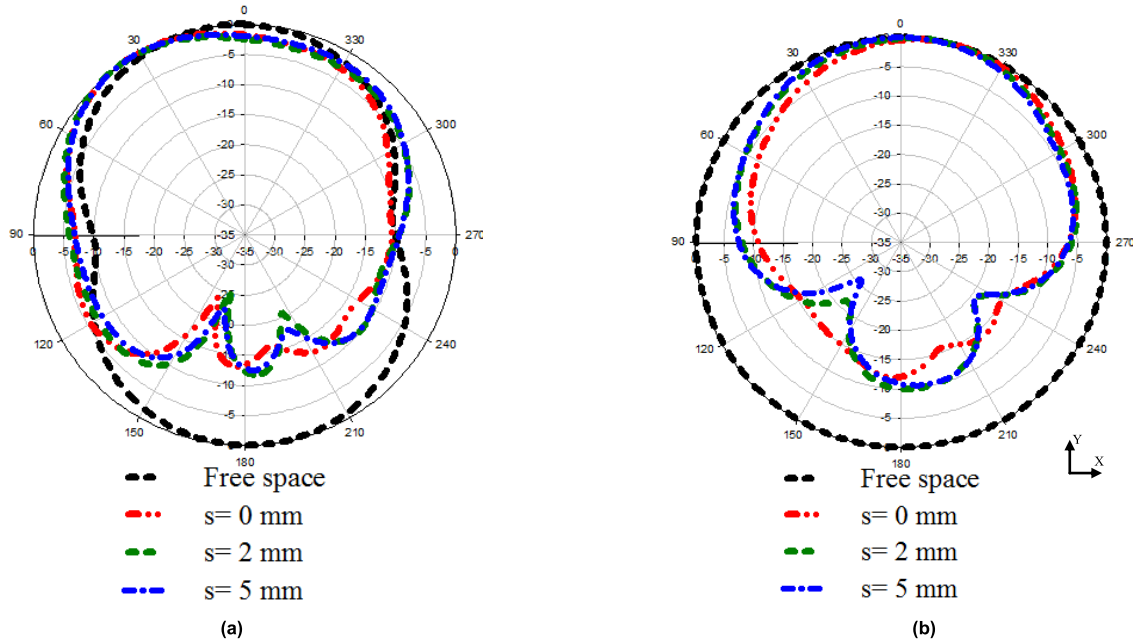

FIGURE 18. Radiation pattern of the CPW antenna alone with varying distance from the multilayer tissue model in the (a) E-plane and (b) H-plane.

between the simulated (Fig. 14(a)) and measured. In addition, the reasonably stable S_{11} is maintained for the three cases (Fig. 15), with S_{11} maintained < -10 dB. The bandwidth of < -10 dB is maintained, similar to the measured case in free space but slightly broadened. Fig. 16(b) shows the result of the antenna alone on the same body positions. It is noticed that the center frequency is affected, shifting to lower frequencies, with the bandwidth slightly widened. These trends are also seen during simulation. The slight widening in the bandwidth in both cases results from degraded quality factors of the radiator element caused by the loading by lossy tissue [35].

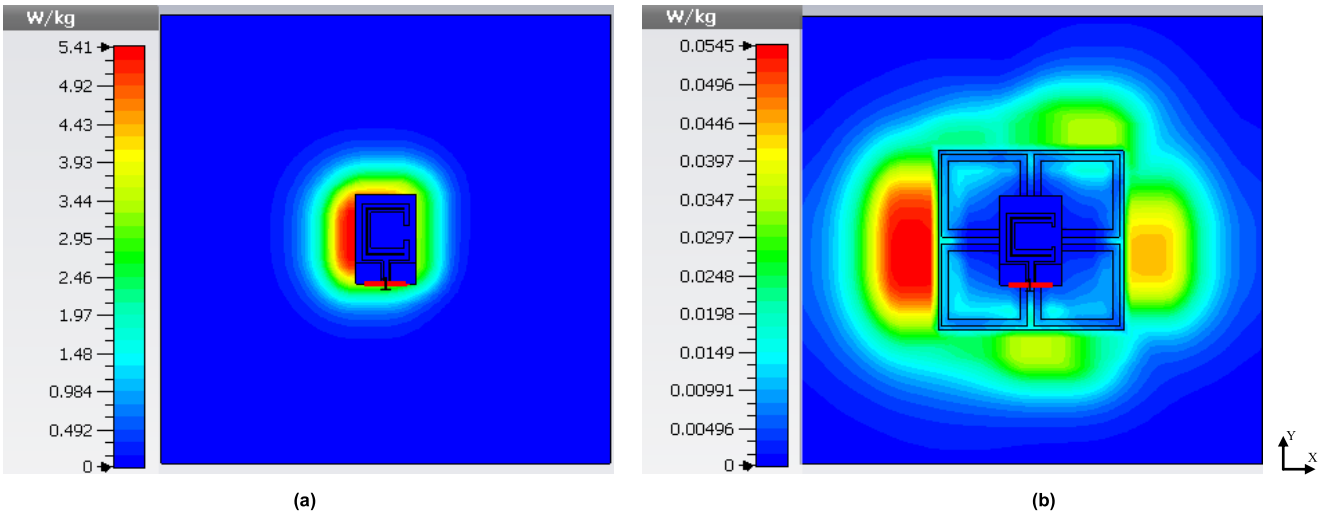

FIGURE 19. SAR investigation for: (a) antenna alone and (b) integrated antenna at 1 mm from the model.

The radiation pattern performance of the antenna with tissue loading, both integrated and on its own, is seen in Fig. 17 and Fig. 18 in the E-plane and the H-plane respectively The same distances as in Fig. 14 are used to study the radiation pattern. For the case of integrated antenna, the FBR is slightly increased compared to the free space case, since the body acts as an extension of the ground planes and directs the radiation far from the body. On the other hand, with the antenna alone and compared with the case of free space, the power absorbed by the body is critical, particularly the backward radiation as seen in Fig. 18. Therefore, the whole radiated power is extremely weak. Based on this result it can be concluded that the EBG isolates the body effectively from the radiation. This means that in the presence of EBG-FSS, the antenna can maintain high efficiency and good impedance matching when placed at different distances, even very close to the human body.

C. SAR EVALUATION

Wearable textile antennas are designed for on-body applications, which means that the antenna must operate near the human body. Thus, SAR is an important factor to calculate when the antenna is excited on the body. SAR values are normally described in units of Watts per kilogram (W/kg).

To investigate the benefits of the EBG-FSS placed between the antenna and the human body, compared with the antenna is alone, a series of SAR simulations were conducted utilizing the human chest model explained in section IV. The model is placed behind the CPW antenna at distances 1, 3 and 5 mm away from the model. Fig. 19 shows the simulated result at 1 mm from the multilayer model. The input power to the antenna is set at 100 mW, and the SAR values determined according to the IEEE C95.1 standards available in the CST MWS software, averaged over 1 g of biological tissue. The SAR levels at 2.4 GHz are summarized in Table 3. A noteworthy drop in SAR is realized by using the EBG-FSS structure,

TABLE 3. SAR values at various distances from the model tissue.

Distance from the phantom (mm)	without EBG-FSS	with EBG-FSS
1	5.41	0.055
3	5.07	0.025
5	4.36	0.015

as the integrated antenna reduced the SAR levels by more than 95%, thus satisfying the standard.

V. CONCLUSION

A compact conformal wearable CPW antenna using EBG-FSS for Medical Body Area Network applications at 2.4 GHz is presented. The antenna and EBG-FSS are designed based on fabric materials that can be integrated with our daily clothes. The antenna was studied in free space, on multilayer model tissues and on a real body. The results show that when an antenna on its own, without EBG-FSS, is loaded by human tissue, the frequency detunes: the antenna performs poorly because of the lossy human tissues. Furthermore, the antenna produces a high value of SAR that exceeds the safety limits, due to its omnidirectional radiation pattern resulting in significant backward radiation.Integrating the CPW antenna with an EBG-FSS structure introduces isolation between the body and the antenna. Thus, the detuning due to human body loading, and also the effects of bending, are significantly reduced. Furthermore, the results reveal that the FBR is improved by 13 dB, the gain by 6.55 dBi and the SAR reduced by more than 95% compared to the antenna alone. Therefore, the presented CPW antenna is fit for future wearable MBAN applications.

REFERENCES

[1] N. A. Malik, M. Ur-Rehman, G. A. Safdar, and Q. H. Abbasi, "Extremely low profile flexible antenna for medical body area networks," in *Proc. IEEE Asia Pacific Microw. Conf. (APMC)*, Nov. 2017, pp. 260–263.

[2] A. Y. I. Ashyap, Z. Z. Abidin, S. H. Dahlan, H. A. Majid, M. R. Kamarudin, and R. A. Abd-Alhameed, "Robust low-profile electromagnetic band-gap-based on textile wearable antennas for medical application," in *Proc. Int. Workshop Antenna Technol., Small Antennas, Innov. Struct., Appl. (iWAT)*, Mar. 2017, pp. 158–161.

[3] H.-B. Li, K.-I. Takizawa, B. Zhen, and R. Kohno, "Body area network and its standardization at IEEE 802.15.MBAN," in *Proc. 16th IST Mobile Wireless Commun. Summit*, Jul. 2007, pp. 1–5.

[4] A. Y. I. Ashyap *et al.*, "Compact and low-profile textile EBG-based antenna for wearable medical applications," *IEEE Antennas Wireless Propag. Lett.*, vol. 16, pp. 2550–2553, 2017.

[5] G. A. Conway and W. G. Scanlon, "Antennas for over-body-surface communication at 2.45 GHz," *IEEE Trans. Antennas Propag.*, vol. 57, no. 4, pp. 844–855, Apr. 2009.

[6] A. Y. I. Ashyap, W. N. N. W. Marzudi, Z. Z. Abidin, S. H. Dahlan, H. A. Majid, and M. R. Kamaruddin, "Antenna incorporated with electromagnetic bandgap (EBG) for wearable application at 2.4 GHz wireless bands," in *Proc. IEEE Asia–Pacific Conf. Appl. Electromagn. (APACE)*, Dec. 2016, pp. 217–221.

[7] H. Cao, V. Leung, C. Chow, and H. Chan, "Enabling technologies for wireless body area networks: A survey and outlook," *IEEE Commun. Mag.*, vol. 47, no. 12, pp. 84–93, Dec. 2009.

[8] A. Y. I. Ashap *et al.*, "Flexible wearable antenna on electromagnetic band gap using PDMS substrate," *TELKOMNIKA*, vol. 15, no. 3, pp. 1454–1460, 2017.

[9] G. Fang, E. Dutkiewicz, M. A. Huq, R. Vesilo, and Y. Yang, "Medical body area networks: Opportunities, challenges and practices," in *Proc. Commun. Inf. Technol. Int. Symp.*, Oct. 2011, pp. 562–567.

[10] B. Lo and G.-Z. Yang, "Body sensor networks—Research challenges and opportunities," in *Proc. IET Seminar Antennas Propag. Body-Centric Wireless Commun.*, Apr. 2007, pp. 26–32.

[11] S.-G. Kim, H.-J. Lee, and J.-G. Yook, "A biomolecular sensing platform using RF active system," *J. Electromagn. Eng. Sci.*, vol. 12, no. 4, pp. 227–233, Dec. 2012.

[12] H. Liu, P. Wen, S. Zhu, B. Ren, X. Guan, and H. Yu, "Quad-band CPW-fed monopole antenna based on flexible pentangle-loop radiator," *IEEE Antennas Wireless Propag. Lett.*, vol. 14, pp. 1373–1376, 2015.

[13] C.-H. Wu, T.-L. Li, M.-H. Hsieh, and J.-S. Sun, "An asymmetric shorted ground using CPW fed antenna for wearable device applications," in *Proc. IEEE Int. Conf. Consum. Electron.-Taiwan (ICCE-TW)*, Jun. 2017, pp. 95–96.

[14] Z. Muhammad, S. M. Shah, Z. Z. Abidin, A. Y. I. Asyhap, S. M. Mustam, and Y. Ma, "CPW-fed wearable antenna at 2.4 GHz ISM band," in *Proc. AIP Conf.*, 2017, vol. 1883, no. 1, p. 020003.

[15] A. Alomainy *et al.*, "Statistical analysis and performance evaluation for on-body radio propagation with microstrip patch antennas," *IEEE Trans. Antennas Propag.*, vol. 55, no. 1, pp. 245–248, Jan. 2007.

[16] N. Haga, K. Saito, M. Takahashi, and K. Ito, "Characteristics of cavity slot antenna for body-area networks," *IEEE Trans. Antennas Propag.*, vol. 57, no. 4, pp. 837–843, Apr. 2009.

[17] M. N. Suma, P. C. Bybi, and P. Mohanan, "A wideband printed monopole antenna for 2.4-GHz WLAN applications," *Microw. Opt. Technol. Lett.*, vol. 48, no. 5, pp. 871–873, May 2006.

[18] P. S. Hall *et al.*, "Antennas and propagation for on-body communication systems," *IEEE Antennas Propag. Mag.*, vol. 49, no. 3, pp. 41–58, Jun. 2007.

[19] S. Yan, P. J. Soh, and G. A. E. Vandenbosch, "Wearable dual-band magneto-electric dipole antenna for WBAN/WLAN applications," *IEEE Trans. Antennas Propag.*, vol. 63, no. 9, pp. 4165–4169, Sep. 2015.

[20] S. Agneessens and H. Rogier, "Compact half diamond dual-band textile HMSIW on-body antenna," *IEEE Trans. Antennas Propag.*, vol. 62, no. 5, pp. 2374–2381, May 2014.

[21] S. Agneessens, S. Lemey, T. Vervust, and H. Rogier, "Wearable, small, and robust: The circular quarter-mode textile antenna," *IEEE Antennas Wireless Propag. Lett.*, vol. 14, pp. 1482–1485, 2015.

[22] S. Yan, P. J. Soh, and G. A. E. Vandenbosch, "Dual-band textile MIMO antenna based on substrate-integrated waveguide (SIW) technology," *IEEE Trans. Antennas Propag.*, vol. 63, no. 11, pp. 4640–4647, Nov. 2015.

[23] R. Moro, S. Agneessens, H. Rogier, and M. Bozzi, "Wearable textile antenna in substrate integrated waveguide technology," *Electron. Lett.*, vol. 48, no. 16, pp. 985–987, Aug. 2012.

[24] Z. Wang, L. Z. Lee, D. Psychoudakis, and J. L. Volakis, "Embroidered multiband body-worn antenna for GSM/PCS/WLAN communications," *IEEE Trans. Antennas Propag.*, vol. 62, no. 6, pp. 3321–3329, Jun. 2014.

[25] W. El Hajj, C. Person, and J. Wiart, "A novel investigation of a broadband integrated inverted-F antenna design; application for wearable antenna," *IEEE Trans. Antennas Propag.*, vol. 62, no. 7, pp. 3843–3846, Jul. 2014.

[26] P. J. Soh, G. A. E. Vandenbosch, S. L. Ooi, and N. H. M. Rais, "Design of a broadband all-textile slotted PIFA," *IEEE Trans. Antennas Propag.*, vol. 60, no. 1, pp. 379–384, Jan. 2012.

[27] K. Kamardin, M. K. A. Rahim, P. S. Hall, N. A. Samsuri, T. A. Latef, and M. H. Ullah, "Planar textile antennas with artificial magnetic conductor for body-centric communications," *Appl. Phys. A, Mater. Sci. Process.*, vol. 122, no. 4, p. 363, 2016.

[28] S. Zhu and R. Langley, "Dual-band wearable textile antenna on an EBG substrate," *IEEE Trans. Antennas Propag.*, vol. 57, no. 4, pp. 926–935, Apr. 2009.

[29] G.-P. Gao, B. Hu, S.-F. Wang, and C. Yang, "Wearable circular ring slot antenna with EBG structure for wireless body area network," *IEEE Antennas Wireless Propag. Lett.*, vol. 17, no. 3, pp. 434–437, Mar. 2018.

[30] S. Velan *et al.*, "Dual-band EBG integrated monopole antenna deploying fractal geometry for wearable applications," *IEEE Antennas Wireless Propag. Lett.*, vol. 14, pp. 249–252, 2015.

[31] Z. H. Jiang, Z. Cui, T. Yue, Y. Zhu, and D. H. Werner, "Compact, highly efficient, and fully flexible circularly polarized antenna enabled by silver nanowires for wireless body-area networks," *IEEE Trans. Biomed. Circuits Syst.*, vol. 11, no. 4, pp. 920–932, Aug. 2017.

[32] H. R. Raa, A. I. Abbosh, H. M. Al-Rizzo, and D. G. Rucker, "Flexible and compact AMC based antenna for telemedicine applications," *IEEE Trans. Antennas Propag.*, vol. 61, no. 2, pp. 524–531, Feb. 2013.

[33] M. Wang *et al.*, "Investigation of SAR reduction using flexible antenna with metamaterial structure in wireless body area network," *IEEE Trans. Antennas Propag.*, vol. 66, no. 6, pp. 3076–3086, Jun. 2018.

[34] M. A. B. Abbasi, S. S. Nikolaou, M. A. Antoniades, M. N. Stevanović, and P. Vryonides, "Compact EBG-backed planar monopole for BAN wearable applications," *IEEE Trans. Antennas Propag.*, vol. 65, no. 2, pp. 453–463, Feb. 2017.

[35] Z. H. Jiang, D. E. Brocker, P. E. Sieber, and D. H. Werner, "A compact, low-profile metasurface-enabled antenna for wearable medical body-area network devices," *IEEE Trans. Antennas Propag.*, vol. 62, no. 8, pp. 4021–4030, Aug. 2014.

[36] S. Yan, P. J. Soh, and G. A. E. Vandenbosch, "Low-profile dual-band textile antenna with artificial magnetic conductor plane," *IEEE Trans. Antennas Propag.*, vol. 62, no. 12, pp. 6487–6490, Dec. 2014.

[37] *CST Microwave Studio*. Accessed: Oct. 10, 2016. [Online]. Available: http/www.cst.com

[38] M. S. Alam, M. T. Islam, and N. Misran, "A novel compact split ring slotted electromagnetic bandgap structure for microstrip patch antenna performance enhancement," *Prog. Electromagn. Res.*, vol. 130, pp. 389–409, 2012.

[39] S. M. Amjadi and M. Soleimani, "A novel compact artificial magnetic conductor based on multiple non-grounded vias," *PIERS Online*, vol. 2, no. 6, pp. 672–675, 2006.

[40] D. Ferreira, R. F. Caldeirinha, I. Cuiñas, and T. R. Fernandes, "Square loop and slot frequency selective surfaces study for equivalent circuit model optimization," *IEEE Trans. Antennas Propag.*, vol. 63, no. 9, pp. 3947–3955, Sep. 2015.

[41] Z. L. Wang, K. Hashimoto, N. Shinohara, and H. Matsumoto, "Frequency-selective surface for microwave power transmission," *IEEE Trans. Microw. Theory Techn.*, vol. 47, no. 10, pp. 2039–2042, Oct. 1999.

[42] F. Yang and Y. Rahmat-Samii, *Electromagnetic Band Gap Structures in Antenna Engineering*. Cambridge, U.K.: Cambridge Univ. Press, 2009.

[43] C. L. Holloway and E. F. Kuester, "Net and partial inductance of a microstrip ground plane," *IEEE Trans. Electromagn. Compat.*, vol. 40, no. 1, pp. 33–46, Feb. 1998.

[44] L. Yang, M. Fan, F. Chen, J. She, and Z. Feng, "A novel compact electromagnetic-bandgap (EBG) structure and its applications for microwave circuits," *IEEE Trans. Microw. Theory Techn.*, vol. 53, no. 1, pp. 183–190, Jan. 2005.

[45] A. Aminian, F. Yang, and Y. Rahmat-Samii, "In-phase reflection and EM wave suppression characteristics of electromagnetic band gap ground planes," in *Proc. IEEE Antennas Propag. Soc. Int. Symp.*, vol. 4, Jun. 2003, pp. 430–433.

[46] S. Zhu, "Wearable antennas for personal wireless," Ph.D. dissertation, Dept. Electron. Elect. Eng., Univ. Sheffield, Sheffield, U.K., 2008.

[47] Z. H. Jiang and D. H. Werner, "Robust low-profile metasurface-enabled wearable antennas for off-body communications," in *Proc. 8th Eur. Conf. Antennas Propag. (EuCAP)*, Apr. 2014, pp. 21–24.

ADEL Y. I. ASHYAP received the B.Eng. and M.Eng. degrees in electrical engineering from Universiti Tun Hussein Onn Malaysia in 2012 and 2014, respectively, where he is currently pursuing the Ph.D. degree in electrical engineering. He has authored or co-authored numbers of journals and proceedings. His current research interests include the design of AMC, EBG, and wearable, small, and compact antennas for wireless body area networks. He received the Chancellor Award for his final year project and a number of Gold, Silver, and Bronze medals in international and local competitions.

ZUHAIRIAH ZAINAL ABIDIN received the B.Eng. degree in electrical engineering (electronic) from Universiti Teknologi Malaysia in 2001, the M.Eng. degree in electrical engineering from Kolej Universiti Tun Hussein Onn Malaysia, Johor, Malaysia, in 2003, and the Ph.D. degree from Bradford University, U.K., in 2011. She was currently a Principal Researcher at the Research Center for Applied Electromagnetics, Universiti Tun Hussein Onn Malaysia. She has authored or co-authored numbers of journals and proceedings, including the IEEE Access, IEEE Transactions on Antenna and Propagation, and IEEE AWPL. Her research interests include MIMO antennas, printed microstrip antennas, wearable antennas, electromagnetic bandgap for wireless and mobile, and high-speed digital circuit's applications.

SAMSUL HAIMI DAHLAN received the Ph.D. degree in signal processing and telecommunications from the Universite de Rennes 1, France, in 2012. He has been a Senior Lecturer with the Faculty of Electric and Electronic Engineering, Universiti Tun Hussein Onn Malaysia (UTHM), since 2012. He is currently with the Research Center for Applied Electromagnetics, UTHM, as a Principal Researcher and appointed as the Head of the center in 2015. He has authored or co-authored numbers of journals, including the IEEE Transaction on Electromagnetic Compatibility and IEEE AWPL. His research interests include optical-microwave generators, focusing systems (dielectric lens and transmit array's synthesis), computational electromagnetic technique, namely, the BORFDTD, and material characterizations. He is supervising a number of Ph.D., master's, and bachelor's students and involved in several research projects sponsored by the industry and government agencies.

HUDA A. MAJID received the B.Eng. degree in electrical engineering (telecommunication) and the M.Eng. and Ph.D. degrees in electrical engineering from Universiti Teknologi Malaysia in 2007, 2010, and 2013, respectively. He is currently a Lecturer with the Department of Electrical Engineering Technology, Faculty of Engineering Technology, Universiti Tun Hussein Onn Malaysia. His research interests include design of microstrip antennas, small antennas, reconfigurable antennas, metamaterials structure, metamaterial antennas, and millimeter-wave antennas. He has published over 50 articles in journals and conference papers.

MUHAMMAD RAMLEE KAMARUDIN (M'08–SM'13) received the degree (Hons.) in electrical and telecommunication engineering from Universiti Teknologi Malaysia, Johor Bahru, Malaysia, in 2003, and the M.Sc. degree in communication engineering and the Ph.D. degree in electrical engineering from the University of Birmingham, Birmingham, U.K., in 2004 and 2007, respectively, under the supervision of Emeritus Professor P. Hall. He has been a Senior Lecturer with the Centre for Electronic Warfare, Information and Cyber, Cranfield Defence and Security, Cranfield University, U.K., since 2017. Prior to this appointment, he was an Associate Professor with the Wireless Communication Centre, Universiti Teknologi Malaysia. He holds an H-Index of 21 (SCOPUS) and over 1700 citations (SCOPUS). He has authored a book chapter of a book entitled *Antennas and Propagation for Body-Centric Wireless Communications* and has published over 220 technical papers in journals and proceedings, including the IEEE Transaction on Antennas and Propagation, the IEEE Antennas and Wireless Propagation Letter, the *IEEE Antenna Magazine*, the IEEE Access, the *International Journal of Antennas and Propagation*, *Progress in Electromagnetic Research, Microwave and Optical Technology Letters,* and *Electronics Letters*. His research interests include antenna design for 5G, MIMO antennas, array antenna for beam forming and beam steering, wireless on-body communications, in-body communications (implantable antenna), RF and microwave communication systems, and antenna diversity. He is a member of IET, an Executive Member of Antenna and Propagation, Malaysia Chapter, and a member of the IEEE Antennas and Propagation Society, the IEEE Communication Society, the IEEE Microwave Theory and Techniques Society, and the IEEE Electromagnetic Compatibility Society. He is an Associate Editor of *Electronics Letters* and *IET Microwaves, Antennas and Propagation*, and an Academic Editor for the *International Journal of Antennas and Propagation*.

AKRAM ALOMAINY (M'03–SM'13) received the M.Eng. degree in communication engineering and the Ph.D. degree in electrical and electronic engineering (specialized in antennas and radio propagation) from the Queen Mary University of London (QMUL), London, U.K., in 2003 and 2007, respectively. In 2007, he joined the School of Electronic Engineering and Computer Science, QMUL, where he is currently a Reader with the Antennas and Electromagnetics Research Group and a member of the Centre for Intelligent Sensing, Institute of Bioengineering. He has authored or co-authored a book, five book chapters, and more than 220 technical papers (over 3900 citations and H-index 29) in leading journals and peer reviewed conferences. His current research interests include small and compact antennas for wireless body area networks, radio propagation characterization and modeling, antenna interactions with human body, computational electromagnetic, advanced antenna enhancement techniques for mobile and personal wireless communications, and advanced algorithm for smart and intelligent antenna and cognitive radio system. He is a member of the IET, a fellow of the Higher Education Academy, U.K., and also a College Member for Engineering and Physical Sciences Research, U.K., and its ICT prioritization panels. He was a recipient of the Isambard Brunel Kingdom Award in 2011 for being an outstanding young science and engineering communicator. He was selected to deliver a TEDx talk about the science of electromagnetic and also participated in many public engagement initiatives and festivals. He is also a reviewer for many funding agencies around the world, including the Expert Swiss National Science Foundation Research, the Engineering and Physical Sciences Research Council, U.K., and the Medical Research Council, U.K. He is an elected member of the U.K. International Union of Radio Science (URSI) panel to represent the U.K. interests of URSI Commission B from 2014 to 2017. He has managed to secure various research projects funded by research councils, charities, and industrial partners on projects ranging from fundamental electromagnetic to wearable technologies. He is the lead of Wearable Creativity Research with QMUL and has been invited to participate at the Wearable Technology Show 2015, Innovate U.K. 2015, and also in the recent Wearable Challenge organized by Innovate U.K. IC Tomorrow as a Leading Challenge Partner to support SMEs and industrial innovation.

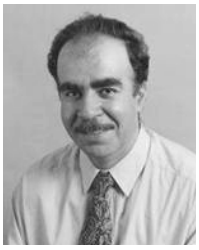

RAED A. ABD-ALHAMEED (M'02–SM'13) is currently a Professor of electromagnetic and radio frequency engineering at the University of Bradford, U.K. He has long years' research experience in the areas of radio frequency, signal processing, propagations, antennas, and electromagnetic computational techniques, and he has published over 500 academic journal and conference papers; in addition, he has co-authored three books and several book chapters. At present, he is the leader of radio frequency, propagation, sensor design, and signal processing, in addition to leading the Communications Research Group for years within the School of Engineering and Informatics, Bradford University, U.K. He is the principal investigator of several funded applications to EPSRCs and a leader of several successful knowledge transfer programmes, such as with Arris (previously known as Pace plc), Yorkshire Water plc, Harvard Engineering plc, IETG Ltd., Seven Technologies Group, Emkay Ltd., and Two World Ltd. He has been also a Research Visitor for Wrexham University, Wales, since 2009, covering the wireless and communications research areas.

His research interests include computational methods and optimizations, wireless and mobile communications, sensor design, EMC, beam steering antennas, energy-efficient PAs, and RF predistorter design applications. He is a fellow of the Institution of Engineering and Technology, a fellow of the Higher Education Academy, and a Chartered Engineer. He received the Business Innovation Award for his successful KTP with Pace and Datong companies on the design and implementation of MIMO sensor systems and antenna array design for service localizations. He is the chair of several successful workshops on Energy Efficient and Reconfigurable Transceivers (EERT): Approach towards Energy Conservation and CO2 Reduction that addresses the biggest challenges for the future wireless systems. He has also been a Co-Investigator in several funded research projects including: 1) H2020 MARIE Skłodowska-CURIE ACTIONS: Innovative Training Networks Secure Network Coding for Next Generation Mobile Small Cells 5G-US; 2) Nonlinear and Demodulation Mechanisms in Biological Tissue (Department of Health, Mobile Telecommunications and Health Research Programme); and 3) Assessment of the Potential Direct Effects of Cellular Phones on the Nervous System (EU: collaboration with six other major research organizations across Europe). He has been as a Guest Editor of the *IET Science, Measurements and Technology Journal* since 2009 and 2012.

JAMAL SULIEMAN KOSHA was born in Tripoli, Libya. He received the B.Sc. degree in electronics and computer engineering from AL Fatah University, Tripoli, in 1994, the M.Sc. degree in communication and computer engineering from Universiti Kebangsaan Malaysia in 2004, and the M.Sc. degree from Human Resources Management, University of Salford, in 2017. He is currently pursuing the Ph.D. degree in wireless and mobile communications systems and its implementation on FPGA with the Faculty of Engineering and Informatics, University of Bradford. He was an Assistant Lecturer for one year with AL Fatah University. He was the Head of the Statistics and Information Office, Almadar Telecom Company, for two years. He was appointed as a Lecturer, the Head of IT Department, and the Deputy Director of the Yafren Higher Institute from 2004 to 2009. He was an Active Member of the National Digital Truncking Network Team in Libya from 2005 to 2007. He was the Head of the Corporate Development Office, Almadar Aljadid Telecom Company, from 2012 to 2015.

JAMES M. NORAS received the B.Sc. degree in physics from St. Andrews University, Scotland, in 1973, the M.Sc. degree in mathematics from Open University, U.K., in 1995, and the Ph.D. degree in semiconductor physics from St. Andrews University in 1978. He is currently a Senior Lecturer with the School of Engineering and Informatics, University of Bradford, U.K. He has published 59 journals and 93 conference papers in fundamental semiconductor physics, analogue and digital circuit design, digital signal processing, and RF system design and evaluation. He is the Director of three internationally franchised B.Eng. courses in electrical and electronic engineering. His main research interests include digital system design and implementation, DSP and coding for communication systems, and localization algorithms for mobile systems. He is a member of the Institute of Physics and a Chartered Physicist.